

## ORIGINAL ARTICLE

# Anaerobic oxidation of methane associated with sulfate reduction in a natural freshwater gas source

Peer HA Timmers<sup>1</sup>, Diego A Suarez-Zuluaga<sup>2</sup>, Minke van Rossem<sup>1</sup>, Martijn Diender<sup>1</sup>, Alfons JM Stams<sup>1,3</sup> and Caroline M Plugge<sup>1,4</sup>

<sup>1</sup>Laboratory of Microbiology, Wageningen University, Wageningen, The Netherlands; <sup>2</sup>Sub-department of Environmental Technology, Wageningen University, Wageningen, The Netherlands; <sup>3</sup>Centre of Biological Engineering, University of Minho, Campus de Gualtar, Braga, Portugal and <sup>4</sup>Wetsus, European Centre of Excellence for Sustainable Water Technology, Leeuwarden, the Netherlands

**The occurrence of anaerobic oxidation of methane (AOM) and trace methane oxidation (TMO) was investigated in a freshwater natural gas source. Sediment samples were taken and analyzed for potential electron acceptors coupled to AOM. Long-term incubations with <sup>13</sup>C-labeled CH<sub>4</sub> (<sup>13</sup>CH<sub>4</sub>) and different electron acceptors showed that both AOM and TMO occurred. In most conditions, <sup>13</sup>C-labeled CO<sub>2</sub> (<sup>13</sup>CO<sub>2</sub>) simultaneously increased with methane formation, which is typical for TMO. In the presence of nitrate, neither methane formation nor methane oxidation occurred. Net AOM was measured only with sulfate as electron acceptor. Here, sulfide production occurred simultaneously with <sup>13</sup>CO<sub>2</sub> production and no methanogenesis occurred, excluding TMO as a possible source for <sup>13</sup>CO<sub>2</sub> production from <sup>13</sup>CH<sub>4</sub>. Archaeal 16S rRNA gene analysis showed the highest presence of ANME-2a/b (ANAerobic METHane oxidizing archaea) and AAA (AOM Associated Archaea) sequences in the incubations with methane and sulfate as compared with only methane addition. Higher abundance of ANME-2a/b in incubations with methane and sulfate as compared with only sulfate addition was shown by qPCR analysis. Bacterial 16S rRNA gene analysis showed the presence of sulfate-reducing bacteria belonging to SEEP-SRB1. This is the first report that explicitly shows that AOM is associated with sulfate reduction in an enrichment culture of ANME-2a/b and AAA methanotrophs and SEEP-SRB1 sulfate reducers from a low-saline environment.**

*The ISME Journal* (2016) 10, 1400–1412; doi:10.1038/ismej.2015.213; published online 4 December 2015

## Introduction

Anaerobic methane oxidation (AOM) coupled to sulfate reduction (SR) was first discovered to occur in marine sediments (Martens and Berner, 1974; Reeburgh, 1976). The process was found to be catalyzed by communities of anaerobic methanotrophic archaea (ANME) and sulfate-reducing bacteria (SRB) of the *Deltaproteobacteria* (Hinrichs *et al.*, 1999; Boetius *et al.*, 2000; Orphan *et al.*, 2001a,b). More recently, AOM was also reported to be coupled to other electron acceptors besides sulfate. In freshwater environments, AOM was coupled to the reduction of nitrate and nitrite (Raghoebarsing *et al.*, 2006; Ettwig *et al.*, 2008, 2009; Hu *et al.*, 2009; Deutzmann and Schink 2011; Haroon *et al.*, 2013). Microbial methane oxidation with iron and/or manganese reduction was described in marine sediments (Beal *et al.*, 2009;

Riedinger *et al.*, 2014), brackish sediments (Egger *et al.*, 2015), a terrestrial mud volcano (Chang *et al.*, 2012) and also in freshwater environments (Crowe *et al.*, 2011; Sivan *et al.*, 2011; Amos *et al.*, 2012). Recently, humic acids (HAs) were also hypothesized to act as electron acceptor for AOM (Gupta *et al.*, 2013). AOM coupled to SR in freshwater is likely limited by the low-sulfate concentrations, which are around 10–500 μM (Holmer and Storkholm, 2001).

Sulfate-dependent AOM has been observed in freshwater systems, but the involvement of other electron acceptors could not be excluded. Moreover, the responsible microorganisms were either not analyzed nor conclusively identified (Grossman *et al.*, 2002; van Breukelen and Griffioen, 2004; Eller *et al.*, 2005; Schubert *et al.*, 2011; Segarra *et al.*, 2015). ANME-1-related archaea have been found in a terrestrial subsurface (Takeuchi *et al.*, 2011), but <sup>13</sup>C-labeled carbon dioxide (<sup>13</sup>CO<sub>2</sub>) formation from <sup>13</sup>C-labeled methane (<sup>13</sup>CH<sub>4</sub>) also occurred in control incubation where no electron acceptor was added. This was also the case in other incubation studies (Beal *et al.*, 2009; Sivan *et al.*, 2011; Egger *et al.*, 2015). These observations make it difficult to link ongoing methane oxidation to a particular electron

Correspondence: PHA Timmers, Laboratory of Microbiology, Wageningen University, Dreijenplein 10, Building 316, 6703HB Wageningen, The Netherlands.

E-mail: peer.timmers@wur.nl

Received 13 August 2015; revised 29 September 2015; accepted 6 October 2015; published online 4 December 2015

acceptor. Moreover,  $^{13}\text{CO}_2$  can also be produced during methanogenesis in a process called trace methane oxidation (TMO) (Zehnder and Brock, 1979). TMO was demonstrated to occur in pure cultures of different methanogens (Zehnder and Brock, 1979; Harder, 1997; Moran *et al.*, 2005, 2007), in granular sludge (Zehnder and Brock 1980; Harder 1997; Meulepas *et al.*, 2010) and in freshwater and terrestrial environments (Zehnder and Brock, 1980; Blazewicz *et al.*, 2012). Differentiation between AOM and TMO is difficult for several reasons: (a) both processes can produce  $^{13}\text{CO}_2$  at comparable rates; (b) at elevated methane partial pressure, TMO rates increase (Zehnder and Brock, 1980; Smemo and Yavitt, 2007) while methanogenesis is repressed, which favors SR (Meulepas *et al.*, 2010); and (c) ferrous sulfate addition may result in enhanced TMO rates (Zehnder and Brock, 1980). This means that with elevated  $^{13}\text{CH}_4$  partial pressure and presence of sulfate, an increase in  $^{13}\text{CO}_2$  and sulfide production cannot be taken as evidence for sulfate-dependent AOM unless net methane consumption is demonstrated. Moreover, although there is convincing evidence that anaerobic methane oxidizing archaea (ANME) are capable of net AOM, detecting ANME sequences or cells in mixed communities that perform methanogenesis does not prove that AOM takes place, since ANME could perform methanogenesis as well (Lloyd *et al.*, 2011; Bertram *et al.*, 2013) and as a consequence could perform TMO.

In this study we used long-term incubations (>168 days) with samples taken from a freshwater natural gas source with added  $^{13}\text{CH}_4$  to investigate the occurrence of both TMO during net methanogenesis and AOM. AOM was distinguished from TMO

by simultaneous detection of  $^{13}\text{CH}_4$ ,  $^{12}\text{CH}_4$  (produced during methanogenesis) and  $^{13}\text{CO}_2$ . We investigated the effect of different electron acceptors that possibly might be involved in AOM. Control incubations without addition of methane were carried out to accurately distinguish between net methane oxidation and net methanogenesis. Archaeal community analysis of long-term incubations with methane and sulfate ( $\text{CH}_4+\text{SO}_4^{2-}$ ), sulfate only ( $\text{SO}_4^{2-}$ -only), and methane only ( $\text{CH}_4$ -only) was performed at 323 days of incubation. Incubations with sulfate and with and without methane were monitored for an extended period of 728 days.

## Materials and methods

### Sampling

Samples were taken in spring of 2011 from two natural gas sources in Berkhout, Noord-Holland, The Netherlands ( $52^\circ38'31''\text{N}$ ,  $4^\circ59'49''\text{E}$ ). These gas sources were used for domestic purposes by capturing natural gas from groundwater pockets, using a 30-m long pipe (Figure 1). Different locations were sampled: the effluent of an active gas source ('tank') and the sediment of the ditch where the effluent is collected ('ditch 1'), the sediment of the ditch where the effluent of the storage tank is collected ('ditch 2') and from the sediment inside a gas source that was no longer in use ('tank 2', not in Figure 1). Sediment samples were collected in nitrogen flushed bottles with an inversed pump. In the laboratory, the gas phase of the bottles was flushed with 100% 5.5 grade methane (99.999%) and stored at  $4^\circ\text{C}$  for  $\pm 21$  months. All samples were pooled 1:1:1 (v/v/v) in an anaerobic chamber prior to inoculation.

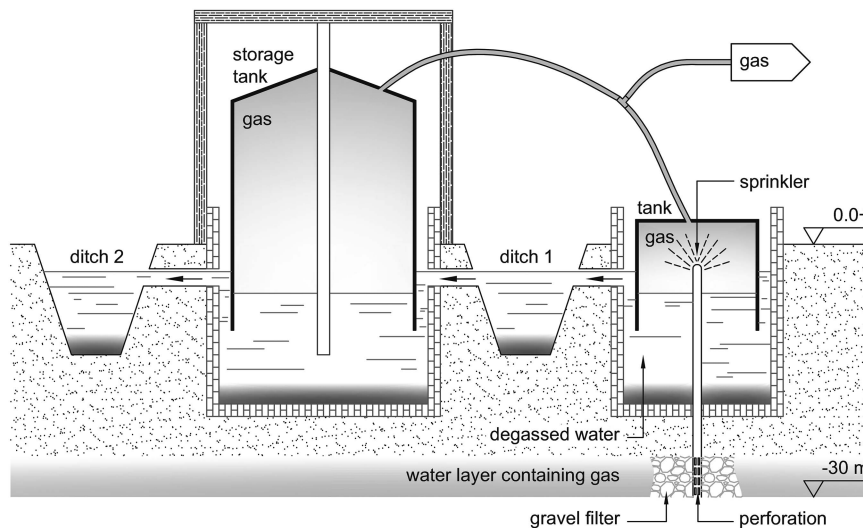


**Figure 1** Schematic representation of the system that is used for capturing natural gas at Berkhout, Noord-Holland, The Netherlands (adapted from Bartstra, 2003). A 30-m deep pipe reaches the pressurized groundwater pockets containing natural gas. Degasification occurs at lower pressure inside the gas source tank where the sprinkler facilitates the process. Gas can be transported to the house or to a storage tank floating on the water ditch. Sampling locations were inside an inactive tank (tank 2, not on picture), from the effluent of the active gas source (tank) and the sediment of the ditch where the effluent is collected (ditch 1) and from the sediment of a ditch where the effluent of the storage tank was collected (ditch 2).

### Media composition

Media were prepared as described previously (Stams *et al.*, 1993) using  $1 \text{ ml l}^{-1}$  of the vitamin stock solution (for composition, see Supplementary Table S1).

### Experimental set-up

Fifteen milliliter aliquots of the pooled sediments ( $0.07 \text{ g}$  volatile suspended solids ( $\text{g}_{\text{VSS}}$ )) were incubated in triplicate in bicarbonate-buffered medium (1:1 v/v) with sulfate ( $20 \text{ mM}$ ), iron (as ferrihydrite,  $10 \text{ mM}$ ), humic acids ( $20 \text{ g l}^{-1}$ ), iron combined with humic acids (iron as ferrihydrite,  $10 \text{ mM}$  and humic acids  $2 \text{ g l}^{-1}$ ) and nitrate ( $20 \text{ mM}$ ). Iron was combined with humic acids to facilitate electron transfer from insoluble iron to soluble humic acids that can act as an electron shuttle (Kappler *et al.*, 2004). A control without electron acceptor was included. All triplicate conditions were tested with and without  $^{13}\text{CH}_4$  in the headspace. All experiments were carried out in  $60 \text{ ml}$  serum bottles closed with butyl rubber stoppers and aluminum caps. After 10 cycles of exchanging the headspace gas with  $\text{N}_2$ , it was changed to  $\text{N}_2/\text{CO}_2$  (1:1) to a pressure of  $1.5 \text{ bar}$ . When  $^{13}\text{CH}_4$  was added,  $\text{N}_2/\text{CO}_2$  was added to a pressure of  $1.3 \text{ bar}$  and  $99.99\%$   $^{13}\text{CH}_4$  gas (Campro Scientific, Veenendaal, The Netherlands) was added to a final pressure of  $1.8 \text{ bar}$ . The serum bottles were incubated at  $15^\circ\text{C}$  in the dark.

### Preparation of ferrihydrite

Ferrihydrite (simplified as  $\text{Fe}(\text{OH})_3$ ) was produced as described for obtaining nanoparticle size ( $<10 \text{ nm}$ ) minerals (Schwertmann and Cornell, 1991). After preparing, the mineral was repeatedly washed and centrifuged for three times and subsequently dialyzed to remove electrolytes. The precipitate was then freeze-dried to remove access water and immediately added to the incubations.

### Analytical measurements

Nitrate and sulfate were analyzed by an ion chromatography system equipped with an Ionpac AS9-SC column and an ED 40 electrochemical detector (Dionex, Sunnyvale, CA, USA). The system was operated at a column temperature of  $35^\circ\text{C}$ , and a flow rate of  $1.2 \text{ ml min}^{-1}$ . Eluent consisted of a carbonate/bicarbonate solution ( $1.8$  and  $1.7 \text{ mM}$ , respectively) in deionized water.

Headspace gas composition was measured on a gas chromatograph-mass spectrometer composed of a Trace GC Ultra (Thermo Fisher Scientific, Waltham, MA, USA) equipped with a Rt-QPLOT column (Restek, Bellefonte, PA, USA), and a DSQ MS (Thermo Fisher Scientific). Helium was used as a carrier gas with a flow rate of  $120 \text{ ml min}^{-1}$  and a split ratio of 60. The inlet temperature was  $80^\circ\text{C}$ , the column temperature was set at  $40^\circ\text{C}$  and the ion source temperature at  $200^\circ\text{C}$ .  $\text{CH}_4$  and  $\text{CO}_2$  in the

headspace were quantified from the peak areas in the gas chromatographs. The fractions of  $^{13}\text{CO}_2$ ,  $^{13}\text{CH}_4$  and  $^{12}\text{CH}_4$  were derived from the mass spectrum as previously done (Shigematsu *et al.*, 2004). Validation of the method was carried out using standards with a known mixture of  $^{13}\text{CO}_2$ ,  $^{12}\text{CO}_2$ ,  $^{13}\text{CH}_4$  and  $^{12}\text{CH}_4$ . The concentrations of total  $\text{CO}_2$ , total  $\text{CH}_4$ ,  $^{13}\text{CO}_2$ ,  $^{12}\text{CH}_4$  (produced during methanogenesis in incubations with  $^{13}\text{CH}_4$ ) and  $^{13}\text{CH}_4$  were calculated as described previously (Timmers *et al.*, 2015). Headspace  $\text{CO}_2$  and  $\text{CH}_4$  after 168 days of incubation was quantified from the peak areas recorded with a CompactGC gas chromatograph (Global Analyser Solutions, Breda, The Netherlands) containing a Carboxen 1010 precolumn, followed by two lines: a Molsieve 5A column (pressure:  $200 \text{ kPa}$ , split flow:  $20 \text{ ml min}^{-1}$ , oven temperature:  $80^\circ\text{C}$ ) and a PDD detector at  $110^\circ\text{C}$ ) and a RT-Q-bond column (pressure:  $150 \text{ kPa}$ , split flow:  $10 \text{ ml min}^{-1}$ , oven temperature:  $80^\circ\text{C}$  with a TCD detector at  $110^\circ\text{C}$ ) with a carrier gas flow of  $10 \text{ ml min}^{-1}$ .

The concentrations of iron(II) and iron(III) were measured with the ferrozine colorimetric method (Stookey, 1970). Prior to analysis, samples were acidified with  $2 \text{ M HCl}$  (1:1 v/v) and centrifuged for  $5 \text{ min}$  at  $15700 \text{ r.c.f.}$  to precipitate humic acids. Absorbance at  $562 \text{ nm}$  was measured in a U-1500 spectrophotometer (Hitachi, Chiyoda, Tokyo, Japan).

Sulfide concentration was measured with the methylene-blue colorimetric method. Samples were directly diluted 1:1 (v/v) in a  $5\%$  (w/v) zinc acetate solution to bind all sulfide. Deionized water was added to a volume of  $4.45 \text{ ml}$  and  $500 \mu\text{l}$  of reagent A ( $2 \text{ g l}^{-1}$  dimethylparaphenylenediamine and  $200 \text{ ml l}^{-1}$   $\text{H}_2\text{SO}_4$ ) and  $50 \mu\text{l}$  of reagent B ( $1 \text{ g l}^{-1}$   $\text{Fe}(\text{NH}_4)(\text{SO}_4)_2 \cdot 12 \text{ H}_2\text{O}$  and  $0.2 \text{ ml l}^{-1}$   $\text{H}_2\text{SO}_4$ ) were added concurrently and mixed immediately. After  $10 \text{ min}$ , samples were measured with a Spectroquant Multy colorimeter (Merck Millipore, Darmstadt, Germany) at  $660 \text{ nm}$ .

Inductively coupled plasma-optical emission spectroscopy using a Vista-MPX CCD simultaneous (Varian Inc., Palo Alto, CA, USA) was used to quantify the elemental composition of all samples, as previously done (Hageman *et al.*, 2013). The standard deviation in all measurements was  $\leq 1.8\%$ .

The pressure of the serum vials was determined using a portable membrane pressure unit GMH 3150 (Greisinger electronic GmbH, Regenstauf, Germany). The pH was checked by pH paper. Conductivity was measured using a standard electrode. The VSS contents were analyzed according to the standard methods (Clesceri *et al.*, 1995).

### DNA extraction

Genomic DNA was extracted from samples after 323 days of incubation from the triplicate incubations with methane and sulfate ( $\text{CH}_4+\text{SO}_4^{2-}$ ), sulfate only ( $\text{SO}_4^{2-}$ -only), and methane only ( $\text{CH}_4$ -only) and from the original sediment (BHori). DNA was



extracted in triplicate for every separate incubation using the Fast DNA Kit for Soil (MP Biomedicals, Santa Ana, CA, USA) according to the manufacturer's protocol with two 45-s beat beating steps using a Fastprep Instrument (MP Biomedicals). Triplicate extracted DNA for every separate incubation was pooled and DNA concentrations were determined with the Qubit 2.0 fluorometer (Thermo Fisher Scientific).

#### Bacterial community profiling

Extracted DNA was subjected to barcoded amplification of the V1–V2 region of the 16S rRNA gene. A PCR amplification replicate of BHori (BHoriA and BHoriB) was carried out to correct for technical biases. Barcoded amplification was carried out using forward primer 27F-DegS (van den Bogert *et al.*, 2011) that was extended with the titanium adapter A and an eight-base sample specific barcode (Hamady *et al.*, 2008) at the 5'-end, and an equimolar mix of reverse primers 338R-I and 338R-II (Daims *et al.*, 1999) that were appended with the titanium adapter B at the 5'-end. All primers are listed in Supplementary Table S2. PCR amplification was performed in a thermocycler GS0001 (Gene Technologies, Braintree, UK) in a total volume of 100 µl containing 2 µl DNA (20 ng µl<sup>-1</sup>), 500 nM of barcoded forward primer and reverse primermix (Biolegio BV, Nijmegen, The Netherlands), 2 U of Phusion Hot start II High-Fidelity DNA polymerase (Finnzymes, Vantaa, Finland), 20 µl of 5 × HF buffer, 2 µl PCR grade nucleotide mix (Roche Diagnostics GmbH, Mannheim, Germany) and 65 µl nuclease-free sterile water (Promega Corporation, Madison, WI, USA). PCR amplification conditions consisted of a pre-denaturing step of 3 min at 98 °C followed by 30 cycles of 98 °C for 10 s, 56 °C for 20 s and 72 °C for 20 s. Lastly, a post-elongation step of 10 min at 72 °C was carried out. PCR products were purified using a GeneJet PCR purification kit (Thermo Fisher Scientific) and the concentration was determined using the Qubit 2.0 fluorometer (Thermo Fisher Scientific). All samples for pyrosequencing were mixed in equimolar amounts. Pooled samples were loaded on a 1% (v/v) agarose gel containing 1 × SYBR Safe (Invitrogen, Thermo Fisher Scientific) and bands of approximately 340 bp were excised and purified with the GeneJet Gel Extraction Kit (Thermo Fisher Scientific) using 25 µl elution buffer for collecting the amplified DNA. Mixed samples were quantified using the Qubit 2.0 fluorometer (Thermo Fisher Scientific) and submitted for pyrosequencing on the 454 Life Sciences GS-FLX platform using Titanium sequencing chemistry (GATC Biotech AG, Konstanz, Germany).

#### Archaea community profiling

Extracted DNA was subjected to barcoded amplification of the 16S rRNA gene. A PCR amplification

replicate of BHori (BHoriA and BHoriB) was carried out to correct for technical biases. A method adapted from Jaeggi *et al.* (2014) was used. Barcoded amplification of 16S rRNA genes was carried out by using forward primer 340F (Gantner *et al.*, 2011) that was extended with the titanium adapter A and a 10-base sample specific barcode at the 5'-end, and reverse primer 1000R (Gantner *et al.*, 2011) that was appended with the titanium adapter B at the 5'-end. All primers are listed in Supplementary Table S2. PCR amplification was performed in a total volume of 50 µl containing 1 µl DNA, 200 nM of each forward and reverse primer (Biolegio BV), 1 U of KOD Hot Start DNA Polymerase (Merck Millipore), 5 µl of 10 × KOD-buffer, 3 µl MgSO<sub>4</sub> (25 mM), 5 µl dNTP mix (2 mM each) and 33 µl nuclease free sterile water. PCR amplification conditions were a pre-denaturing step at 95 °C for 2 min followed by 35 cycles of 95 °C for 20 s, 5 °C for 10s, and 70 °C for 15 s. The approximately 660 bp PCR amplicon was subsequently purified using the MSB Spin PCR apace kit (STRATEC Biomedical AG, Birkenfeld, Germany) and the concentration was checked with a Nanodrop 1000 spectrophotometer (Thermo Fisher Scientific). Purified PCR products were mixed in equimolar amounts. The mixed sample was further purified using the Purelink PCR Purification kit (Thermo Fisher Scientific), with high-cutoff binding buffer B3, and submitted for pyrosequencing on the 454 Life Sciences GS-FLX platform using Titanium sequencing chemistry (GATC Biotech AG).

#### Pyrosequencing analysis

The pyrosequencing data were analyzed with a workflow based on Quantitative Insights Into Microbial Ecology (QIIME) v1.2 (Caporaso *et al.*, 2010), and reads were filtered for chimeric sequences using the USEARCH algorithm. Operational taxonomic unit (OTU) clustering was performed with settings as recommended in the QIIME newsletter of 17 December 2010 (<http://qiime.wordpress.com/2010/12/17/new-default-parameters-for-uclust-otu-pickers/>) using an identity threshold of 97%. The SILVA reference database was used for taxonomic classification (Quast *et al.*, 2013). After picking representative OTUs, the relative amount of reads of every OTU to the total amount of reads per sample was quantified. Afterwards, the average relative amount of reads per condition from the biological triplicate samples was calculated. For analysis of the original sample BHori, the average of the PCR duplicates (BHoriA and BHoriB) was calculated. Then, the significant differences of every representative OTU between the conditions CH<sub>4</sub>+SO<sub>4</sub><sup>2-</sup> and CH<sub>4</sub>-only and between CH<sub>4</sub>+SO<sub>4</sub><sup>2-</sup> and SO<sub>4</sub><sup>2-</sup>-only were calculated separately, using the Kruskal–Wallis test ( $P < 0.05$ ). For archaea, we then selected only representative OTUs that were significantly higher in conditions with CH<sub>4</sub>+SO<sub>4</sub><sup>2-</sup> as separately compared with CH<sub>4</sub>-only and SO<sub>4</sub><sup>2-</sup>-only. For bacteria, we selected only representative OTUs

that were significantly higher in conditions with  $\text{CH}_4 + \text{SO}_4^{2-}$  as compared with both  $\text{CH}_4$ -only and  $\text{SO}_4^{2-}$ -only.

#### Quantitative real-time PCR

Extracted genomic DNA was used for qPCR analysis. The DNA was purified with the DNA clean and concentrator-5 kit (Zymo Research, Irvine, CA, USA) and the concentration was determined with the Qubit 2.0 fluorometer (Thermo Fisher Scientific). Amplifications with specific primers for ANME-2a/b were carried out as described previously (Timmers *et al.*, 2015). Quantification was expressed as the total number of 16S rRNA gene copies per  $\text{g}_{\text{vss}}$  extracted from the incubations.

#### Nucleotide sequences

Nucleotide sequence data reported are available in the DDBJ/EMBL/GenBank databases under the accession numbers LN795911–LN796465 for archaeal sequences and LN796466–LN808676 for bacterial sequences.

## Results and discussion

### Trace methane oxidation

Methane production was observed in most conditions, but was negligible in the presence of sulfate and did not occur in the presence of nitrate (Figure 2). Methane production in conditions with and without added methane showed a similar pattern, but the amount of methane produced was lower in incubations where methane was added (Supplementary Figure S1A). This was probably caused by the increase of TMO due to a higher methane concentration (Zehnder and Brock, 1980; Smemo and Yavitt, 2007). Production of  $^{13}\text{CO}_2$  was apparent in all incubations with  $^{13}\text{CH}_4$  in the headspace, except in the conditions with nitrate and HAs (Figure 2 and Supplementary Figure S1B). Typical for TMO,  $^{13}\text{CO}_2$  simultaneously increased with methane formation in the conditions with ferrihydrite, ferrihydrite + HAs and the control without electron acceptor (Figure 2). The  $^{13}\text{CO}_2$  production was not substantially different between ferrihydrite, ferrihydrite + HAs and the control conditions (Wilcoxon rank-sum test,  $P < 0.05$ ; Table 1), indicating that TMO was not influenced by the electron

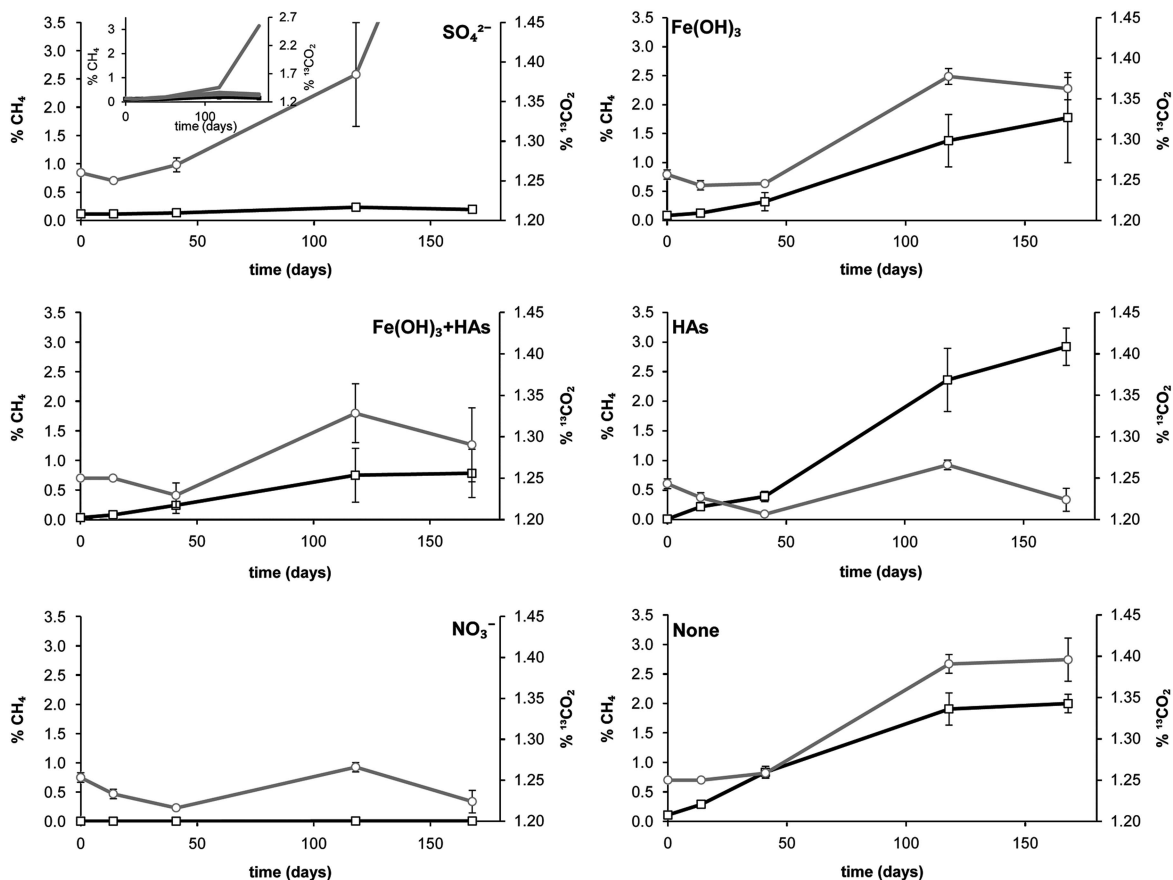


**Figure 2** Percentage of methane (black lines) and percentage of  $^{13}\text{CO}_2$  of total  $\text{CO}_2$  during 168 days of incubation in bottles with 100%  $^{13}\text{CH}_4$  in the headspace and with different electron acceptors. Standard deviations represent triplicate incubations. Note the different scale in the condition with sulfate where one of the triplicates '1A-2' highly increased in  $^{13}\text{CO}_2$ .

acceptors added. When ferrihydrite was added, the  $^{13}\text{CO}_2$  production continued when all iron was reduced to Fe(II) after 300 days, without addition of HAs (Supplementary Figure S2). Iron reduction did occur faster in incubations with ferrihydrite + HAs than in the incubations with only ferrihydrite. The incubations with  $20\text{ g l}^{-1}$  HAs contained an average of  $28.8 (\pm 1.0)$  mM acid soluble Fe(II) after 300 days of incubation and did not show any detectable  $^{13}\text{CO}_2$  increase (Figure 2, Supplementary Figure S1B and Table 1). The HAs batch used contained calcium which could scavenge produced  $\text{CO}_2$  to form calcium carbonate. After acidification of the samples, an increase in total  $\text{CO}_2$  was observed but the percentage of  $^{13}\text{CO}_2$  did not increase. It was reported that reduced methane emission after addition of HAs to peat ecosystems could be caused by increased methane oxidation (Blodau and Deppe, 2012). In contrast, here we observed higher methane production after addition of HAs but no methane oxidation.

#### Anaerobic methane oxidation

Only in the incubations with sulfate, an increase in  $^{13}\text{CO}_2$  with no increase in  $^{12}\text{CH}_4$  was observed (Figure 2). The ratio of methane oxidized per methane produced was only  $>1$  for conditions with sulfate, which is indicative for AOM (Table 1). In previous studies, sulfate addition inhibited methane formation and thus  $^{13}\text{CO}_2$  production from TMO in freshwater sludge (Zehnder and Brock, 1980; Meulepas *et al.*, 2010) and in freshwater slurries (Segarra *et al.*, 2013) and only stimulated methane oxidation in brackish water slurries (Segarra *et al.*, 2013). In our study, the pooled inoculum contained

**Table 1**  $\text{CH}_4$  oxidized per  $\text{CH}_4$  formed after 168 days of incubation as calculated from the amount of  $^{12}\text{CH}_4$  formed and the amount of  $^{13}\text{CO}_2$  formed in incubations with a headspace of 100%  $^{13}\text{CH}_4$  with different electron acceptors

Condition	Bottle #	Total $\text{CO}_2$ formed ( $\mu\text{mol}$ )	$^{13}\text{CO}_2$ formed ( $\mu\text{mol}$ )	$^{12}\text{CH}_4$ formed ( $\mu\text{mol}$ )	$\text{CH}_4$ oxidized/ $\text{CH}_4$ formed
$\text{SO}_4^{2-}$	1A-1	432.3	6.2	1.8	$>1$
	1A-2	108.9	20.3	1.5	$>1$
	1A-3	532.7	10.4	0.9	$>1$
$\text{Fe}(\text{OH})_3$	2A-1	0	2.2	14.8	0.15
	2A-2	209.4	4.8	34.5	0.14
	2A-3	433.3	8.1	41.7	0.19
$\text{Fe}(\text{OH})_3$ +HAs	3A-1	0	1.5	13.8	0.11
	3A-2	23.0	2.5	19.6	0.13
	3A-3	0	0	5.8	n/a
HAs	4A-1	0	0	51.4	n/a
	4A-2	0	0	56.0	n/a
	4A-3	0	0	47.4	n/a
$\text{NO}_3^-$	5A-1	0	0	0.0	n/a
	5A-2	0	0.2	0.0	n/a
	5A-3	0	0	0.0	n/a
None	6A-1	283.0	6.8	33.0	0.21
	6A-2	159.3	6.1	34.9	0.18
	6A-3	36.2	4.3	37.5	0.11

n/a, not applicable.

an average of around 2 mM sulfate (Supplementary Table S3). All sulfate was reduced after 41 days of incubation and methanogenesis continued in most conditions, which was accompanied by continued  $^{13}\text{CO}_2$  production during TMO (Figure 2). Only where sulfate was added, sulfate addition stimulated methane oxidation and repressed methane production, indicating AOM coupled to SR at low salinity. AOM could not be coupled to any other electron acceptor than sulfate. Inductively coupled plasma measurements of all samples prior to mixing showed that only sulfur and iron were present, which in oxidized form could be possible electron acceptors for AOM, whereas the amount of selenium and manganese was not significant (Supplementary Table S4). In incubations with nitrate and humic acids, no  $^{13}\text{CO}_2$  was produced.

Reduction of the electron acceptors sulfate, ferrihydrite and nitrate occurred in all conditions with and without addition of methane (Table 2). The reduction rates of sulfate with and without added methane in the first 168 days were similar (two-tailed *t*-test with unequal variance,  $P < 0.05$ ), which was probably due to endogenous SR masking sulfate-dependent AOM. After 343 days of incubation, the SR rate in incubations with only sulfate had substantially decreased due to endogenous substrate depletion whereas in conditions with methane and sulfate, there was no difference in SR rates. However, in this time period AOM could not be linked to SR and sulfide production as the abundant green sulfur bacteria *Chlorobiaceae* (Supplementary Figure S3)

**Table 2** Reduction rates of the electron acceptors sulfate, iron in the form of ferrihydrite with and without humic acids (HAs) and nitrate in each incubation with and without methane in the headspace during the first 168 days of incubation and sulfate reduction rates in incubations with sulfate between 343 and 728 days of incubation (in  $\mu\text{mol g}_{\text{VSS}}^{-1} \text{day}^{-1}$ ). Standard deviations represent biological triplicates

Condition	Reduction rates ( $\mu\text{mol g}_{\text{VSS}}^{-1} \text{day}^{-1}$ )
<i>Sulfate</i>	
0–168 days	
$\text{CH}_4 + \text{SO}_4^{2- \text{ac}}$	5.14 ( $\pm 3.04$ )
$\text{SO}_4^{2- \text{a}}$	7.58 ( $\pm 0.50$ )
$\text{CH}_4^{\text{b}}$	0
343–728 days	
$\text{CH}_4 + \text{SO}_4^{2- \text{ac}}$	5.94 ( $\pm 0.83$ )
$\text{SO}_4^{2- \text{c}}$	5.02 ( $\pm 0.16$ )
<i>Iron</i>	
0–168 days	
$\text{CH}_4 + \text{Ferrihydrite}^{\text{a}}$	0.12 ( $\pm 0.01$ )
Ferrihydrite <sup>a</sup>	0.15 ( $\pm 0.02$ )
$\text{CH}_4 + \text{Ferrihydrite} + \text{HAs}^{\text{b}}$	10.58 ( $\pm 1.95$ )
Ferrihydrite+HAs <sup>b</sup>	4.29 ( $\pm 7.10$ )
<i>Nitrate</i>	
$\text{CH}_4 + \text{NO}_3^-^{\text{a}}$	28.02 ( $\pm 1.38$ )
$\text{NO}_3^-^{\text{a}}$	25.32 ( $\pm 1.02$ )

Means with different letters in superscript are significant (independent two-tailed *t*-test with unequal variance,  $P < 0.05$ ).

could have caused the fluctuations in sulfide levels. Growth and activity of *Chlorobiaceae* explained the green coloration occurring specifically in incubations amended with sulfate, which derived from the bacteriochlorophyll of green sulfur bacteria (Gorlenko, 1970). Green sulfur bacteria are strictly anaerobic autotrophic sulfide oxidizers and have been found to be active when exposed to very little light (Beatty *et al.*, 2005; Manske *et al.*, 2005), which could explain activity even in the dark with limited exposure to light during sampling of our incubations. Their activity probably kept the sulfide concentration low. After maintaining complete darkness in the slurries, the  $^{13}\text{CO}_2$  production continued throughout incubation time and free sulfide was eventually measured. In bottle 1A-2 that showed the highest  $^{13}\text{CO}_2$  production after 168 days of incubation (Table 1), sulfide production increased simultaneously with  $^{13}\text{CO}_2$  production during the last period between 343 and 728 days (Supplementary Figure S4). This shows that at long term, net methane oxidation accompanied sulfide production.

#### Microbial community profiling

Microbial community profiling was only carried out on triplicates of the conditions  $\text{CH}_4+\text{SO}_4^{2-}$ ,  $\text{CH}_4$ -only,  $\text{SO}_4^{2-}$ -only, and the original sediment after 323 days of incubation. For all samples that were analyzed, the highest average percentage of 16S rRNA reads for *Archaea* clustered within the *Methanosarcinaceae*, *Methanoregulaceae*, *Methanosaetaceae*, *Methanobacteriaceae*, and the Miscellaneous Crenarchaeota Group (MCG) (Supplementary Figure S5). Archaeal OTUs that showed a significantly higher percentage of reads (Kruskal–Wallis,  $P < 0.05$ ) in condition  $\text{CH}_4+\text{SO}_4^{2-}$ , as compared with  $\text{CH}_4$ -only (Figure 3a) and  $\text{SO}_4^{2-}$ -only (Figure 3b) make up less than 10% of all reads. In condition  $\text{CH}_4+\text{SO}_4^{2-}$ , ANME-2a/b sequences represented 0.16% of all reads and were much more abundant than in the condition  $\text{CH}_4$ -only. Higher abundance of ANME-2a/b in conditions  $\text{CH}_4+\text{SO}_4^{2-}$  compared with  $\text{SO}_4^{2-}$ -only was shown by qPCR analysis (Supplementary Figure S6). This indicates the involvement of ANME-2a/b in AOM coupled to SR, as shown before in marine

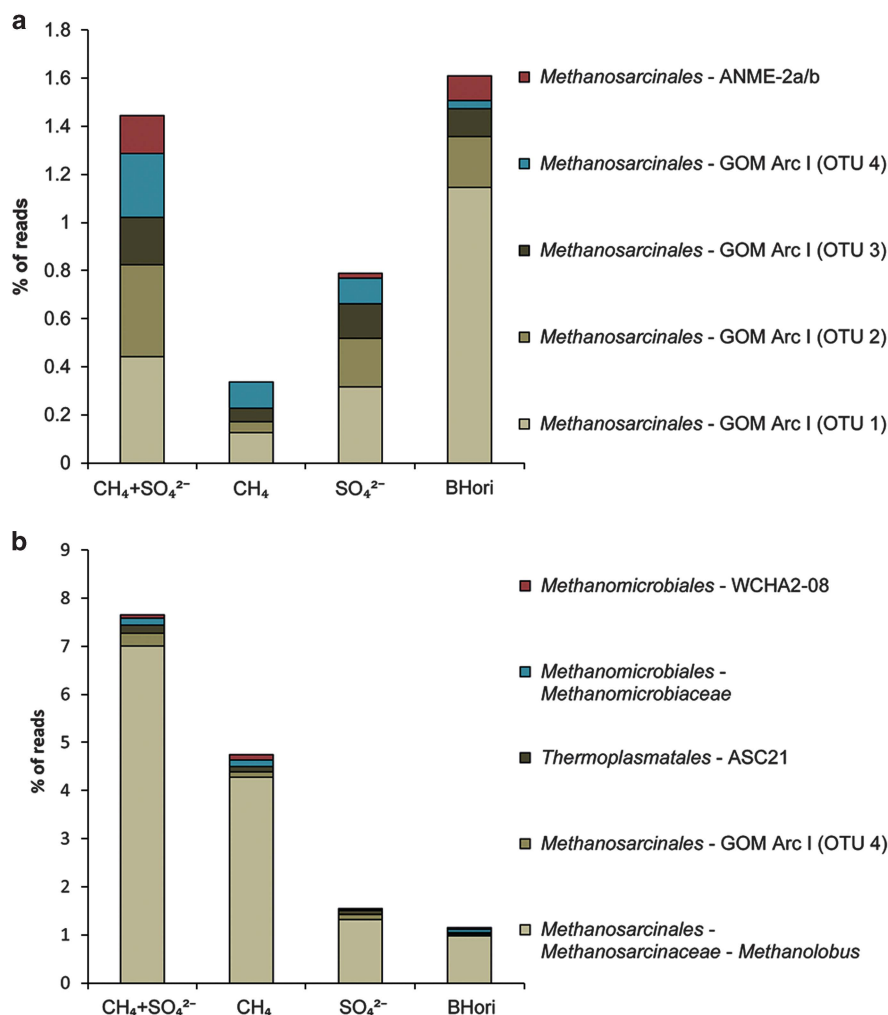


**Figure 3** Archaeal 16S rDNA pyrosequencing results showing the representative OTUs that were significantly higher in the conditions  $\text{CH}_4+\text{SO}_4^{2-}$  as compared with  $\text{CH}_4$ -only (a) and  $\text{SO}_4^{2-}$ -only (b) (Kruskal–Wallis,  $P < 0.05$ ). Also displayed is the original pooled sample (BHori). Displayed is the average percentage of reads per representative OTU of the three biological triplicates per condition.



environments (Orphan *et al.*, 2001a). The ANME-2a/b OTU showed 98% identity with ANME-2a/b from both marine and non-marine environments and do not form a monophyletic cluster with ANME-2a/b found in other low-sulfate environments (Figure 4). A marine enrichment of ANME-2a/b species that share 98% identity was previously shown to be completely inhibited in AOM activity at a salinity of 5‰ (Meulepas *et al.*, 2009), indicating that the ANME-2a/b detected in this study are adapted to low salinity.

A higher percentage of reads was also found for 1 OTU of *Methanosarcinales* GOM Arc I (OTU 4) in conditions CH<sub>4</sub>+SO<sub>4</sub><sup>2-</sup> compared with both CH<sub>4</sub>-only and SO<sub>4</sub><sup>2-</sup>-only (Figure 3). This GOM Arc I group was previously named ‘ANME-2d’ (Mills *et al.*, 2003) but was renamed to ‘GOM Arc I’ since it was not monophyletic with other ANME-2 subtypes and no AOM activity or aggregation with sulfate reducers had been shown (Lloyd *et al.*, 2006). Recently, the name ANME-2d was re-adopted for a cluster that harbors ‘*Ca. Methanoperedens nitroreducens*’, which performed AOM coupled to nitrate reduction (Haroon *et al.*, 2013). This cluster was previously identified in a nitrate-dependent AOM enrichment (Raghoebarsing *et al.*, 2006) and was named ‘AOM associated archaea’ (AAA) (Knittel and Boetius, 2009). The GOM Arc I related OTU 4 found in this study

was 97% identical to ‘*Ca. M. nitroreducens*’ and was 99% identical to other AAA members that were proposed to be responsible for freshwater AOM coupled to SR in Lago di Cadagno sediments (Schubert *et al.*, 2011) (Figure 4). The AAA were also found to be abundant in an aquifer where methane and sulfate were present (Flynn *et al.*, 2013). It was already shown that ‘*Ca. M. nitroreducens*’ uses the complete reverse methanogenesis pathway and it was suggested that the genes for nitrate reduction were obtained from a bacterial donor (Haroon *et al.*, 2013). We did not find nitrate-dependent AOM activity, which leaves open the possibility that the AAA in this study could perform AOM coupled to SR. Sulfate addition in the presence of methane also had a positive effect on other GOM Arc I related OTUs (Figures 3a and 4), which makes a contribution of GOM Arc I to AOM activity likely. The higher percentage of reads of *Methanlobus* in conditions CH<sub>4</sub>+SO<sub>4</sub><sup>2-</sup> compared with SO<sub>4</sub><sup>2-</sup>-only (Figure 3b) implied that methane addition had an effect on *Methanlobus* abundance. The reason for this effect is unclear, since this genus is known to be able to utilize methylated compounds (Zhang *et al.*, 2008), but not methane. However, *Methanlobus* was also found in a marine methane-oxidizing bioreactor (Girguis *et al.*, 2003).

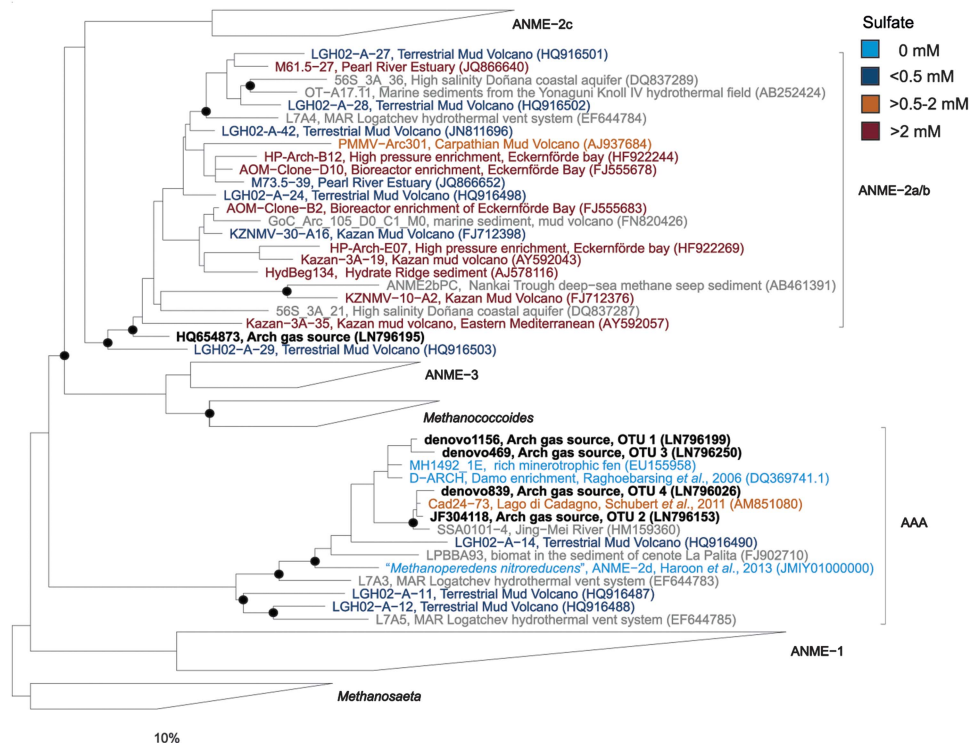


**Figure 4** Phylogenetic tree of archaeal 16S rRNA gene sequences derived from the SILVA SSU Ref database (release 111). The tree was constructed using the ARB neighbor-joining method with terminal filtering and the Jukes–Cantor correction using almost full-length 16S rRNA sequences. Closed circles represent bootstrap values > 70% (1000 replicates). The scale bar represents the percentage of changes per nucleotide position. Short length 16S rRNA sequences (<1000 bp) were afterwards added to the tree using the ARB parsimony method. Color coding represents different sulfate concentrations (mM) of the environments where the sequences were found. Sequences in gray had no clearly reported sulfate data. Sequences found in this study are depicted in black and bold.



Bacterial diversity was high in all samples, with the highest relative number of reads for all samples clustering with the *Deltaproteobacteria* (*Syntrophobacteriacaeca* and *Desulfobacteraceae*) and *Gamma-proteobacteria* (*Methylococcaceae*), *Bacteroidetes*, *Chloroflexi*, *Firmicutes* and *Chlorobi* (family *Chlorobiaceae*) (Supplementary Figure S3). Bacterial OTUs that showed a substantially higher percentage of reads (Kruskal–Wallis,  $P < 0.05$ ) in condition  $\text{CH}_4 + \text{SO}_4^{2-}$  as compared with both  $\text{CH}_4$ -only and  $\text{SO}_4^{2-}$ -only make up less than 0.5% of all reads (Figure 5). These OTUs clustered with the *Desulfobacteraceae*, *Clostridiales* and *Planctomycetaceae*. The OTUs of *Desulfobacteraceae* belonged to the Sva0081 sediment group, *Desulfobacterium* spp. and the SEEP-SRB1 cluster. The latter OTU of SEEP-SRB1 (AB630772) was only found in condition  $\text{CH}_4 + \text{SO}_4^{2-}$ . However, other SEEP-SRB1 OTUs that were detected did not show a difference in read abundance between the conditions  $\text{CH}_4 + \text{SO}_4^{2-}$ ,  $\text{CH}_4$ -only and  $\text{SO}_4^{2-}$ -only. The SEEP-SRB1 clade has been detected in several marine AOM-mediating environments (Orphan *et al.*, 2001b; Knittel *et al.*, 2003; Lösekann *et al.*, 2007; Pernthaler *et al.*, 2008; Harrison *et al.*, 2009; Yanagawa *et al.*, 2011; Vigneron *et al.*, 2013) and enrichments (Jagersma *et al.*, 2009; Zhang *et al.*, 2011). The SEEP-SRB1 OTUs found in this study clustered in undefined subgroups outside the marine SEEP-SRB1 subgroups that were described previously (Figure 6), of which SEEP-SRB1a was identified as the dominant bacterial partner of ANME-2a/b in marine AOM-mediating enrichments (Schreiber *et al.*, 2010). From the other OTUs that showed a higher percentage of reads in condition  $\text{CH}_4 + \text{SO}_4^{2-}$ , little is known about their role in AOM coupled to SR. It has been shown before that different SRB besides SEEP-SRB1 belonging to *Desulfobacteraceae* form consortia with different ANMEs (Orphan *et al.*, 2002; Vigneron *et al.*, 2013)

and even non-SRB were found to aggregate with ANMEs (Pernthaler *et al.*, 2008). We did not find any sequences related to the NC10 phylum of bacteria, harboring the nitrate-dependent methanotrophic bacterium ‘*Ca. Methylopirabilis oxyfera*’ (Ettwig *et al.*, 2010), and we also did not obtain any PCR product using specific primers for this clade (data not shown), which is in line with the lack of AOM coupled to denitrification.

#### AOM at low-sulfate concentrations

The sulfate concentration was 0.07 mM in the gas source effluent and about 2 mM in the pooled inoculum (Supplementary Table S3). The measured conductivity and chloride concentration of the gas source effluent and pooled inoculum samples (Supplementary Table S3) indicate a somewhat higher salinity than typical freshwater, but a much lower salinity than typical brackish environments. This could correspond to the historical marine influence of the adjacent lake (Markermeer) that was formed due to dike construction, as described for proximal sites (van Diggelen *et al.*, 2014). In marine environments, the sulfate:chloride ratio of the lake surface water was around 1:19. The sulfate:chloride ratio of the lake surface water was around 1:2.6, with 1.7 mM sulfate and 4.4 mM chloride (Supplementary Table S3). Therefore, marine influences cannot explain the relatively high-sulfate concentrations. The sulfate concentration in deeper layers of the gas source could be even higher than measured in the gas source effluent before AOM took place. In marine systems, AOM rates started to be affected below 2–3 mM sulfate (Meulepas *et al.*, 2009; Wegener and Boetius, 2009) but occurred even below 0.5 mM of sulfate (Beal *et al.*, 2011; Yoshinaga *et al.*, 2014). In typical freshwater environments, the sulfate concentration is generally lower than 0.5 mM, making

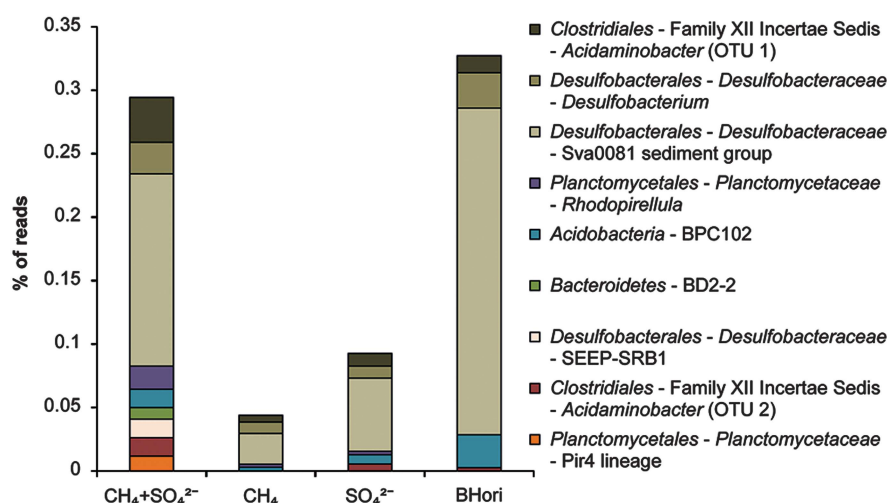


**Figure 5** Bacterial 16S rDNA pyrosequencing results showing the representative OTUs that were significantly higher in the conditions  $\text{CH}_4 + \text{SO}_4^{2-}$  as compared with both  $\text{CH}_4$ -only and  $\text{SO}_4^{2-}$ -only (Kruskal–Wallis,  $P < 0.05$ ). Also displayed is the original pooled sample (BHori). Displayed is the average percentage of reads per representative OTU of the three biological triplicates per condition.

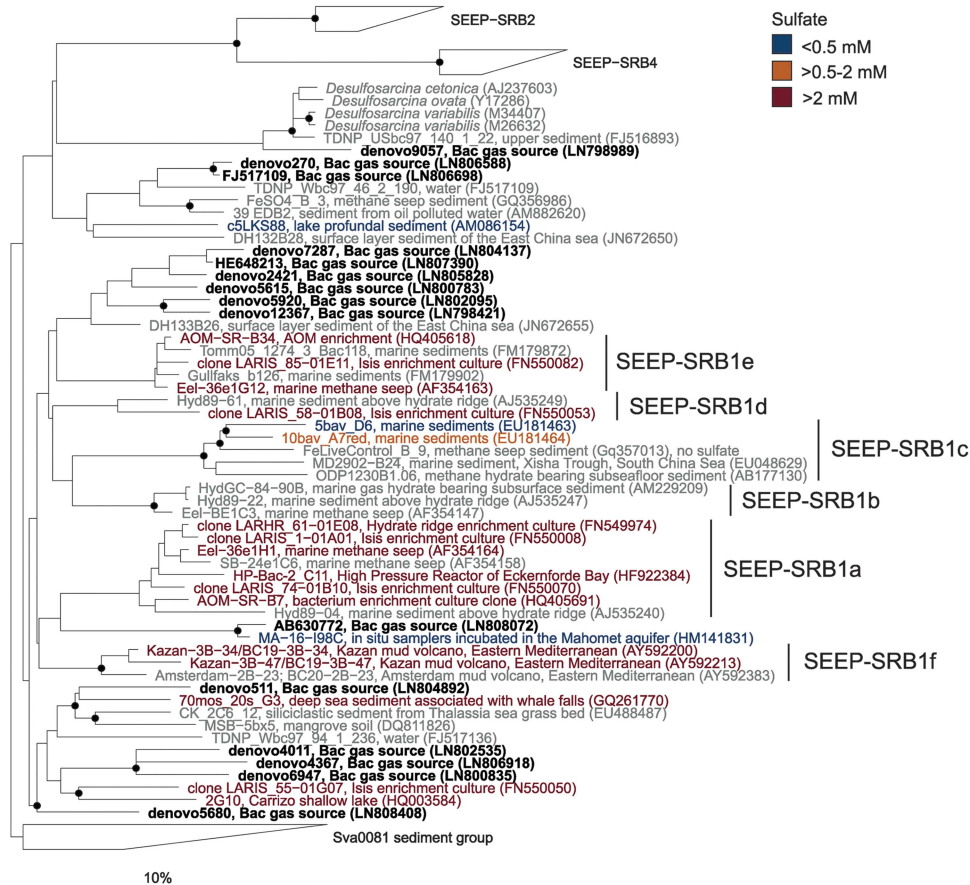


**Figure 6** Phylogenetic tree of bacterial 16S rRNA gene sequences derived from the SILVA SSU Ref database (release 111). The tree was constructed using the ARB neighbor-joining method with terminal filtering and the Jukes-Cantor correction using almost full-length 16S rRNA sequences. Closed circles represent bootstrap values > 70% (1000 replicates). The scale bar represents the percentage of changes per nucleotide position. Short length 16S rRNA sequences (<1000 bp) were afterwards added to the tree using the ARB parsimony method. Color coding represents different sulfate concentrations (mM) of the environments where the sequences were found. Sequences in gray had no clearly reported sulfate data. Sequences found in this study are depicted in black and bold.

AOM-SR feasible but at low rates. AOM in freshwater was recently shown to be a strong methane sink at sulfate concentrations as low as 1.2–0.1 mM (Segarra *et al.*, 2015). Our finding of AOM activity only in conditions with methane and sulfate, and the enrichment of ANME-2a/b and SEEP-SRB1, suggests that these syntrophic clades are ubiquitously distributed in marine and in low-salinity environments and perform AOM at low-sulfate concentrations.

## Conflict of Interest

The authors declare no conflict of interest.

## Acknowledgements

We thank Douwe Bartstra (Vereniging tot Behoud van de Gasbronnen in Noord-Holland, The Netherlands), Carla Frijters (Paques BV, The Netherlands) and Teun Veuskens (Laboratory of Microbiology, WUR, The Netherlands) for sampling; Martin Meirink (Hoogheemraadschap Hollands Noorderkwartier, The Netherlands) for physico-chemical data; Freek van Sambeek for providing Figure 1; Lennart Kleinjans (Laboratory of Microbiology, WUR,

The Netherlands) for help with pyrosequencing analysis, Irene Sánchez-Andrea (Laboratory of Microbiology, WUR, The Netherlands) for proof-reading and Katharina Ettwig (Department of Microbiology, Radboud University Nijmegen, The Netherlands) for providing *M. oxyfera* DNA. We want to thank all anonymous reviewers for valuable contributions. This research is supported by the Dutch Technology Foundation STW (project 10711), which is part of the Netherlands Organization for Scientific Research (NWO), and which is partly funded by the Ministry of Economic Affairs. Research of AJMS is supported by ERC grant (project 323009) and the Gravitation grant (project 024.002.002) of the Netherlands Ministry of Education, Culture and Science and the Netherlands Science Foundation (NWO).

## References

Amos RT, Bekins BA, Cozzarelli IM, Voytek MA, Kirshtein JD, Jones EJ *et al.* (2012). Evidence for iron-mediated anaerobic methane oxidation in a crude oil-contaminated aquifer. *Geobiology* **10**: 506–517.  
 Bartstra D. (2003). Gasbronnen in Noord-Holland. *Vereniging tot behoud van gasbronnen in Noord-Holland, Middenbeemster, Netherlands* ISBN 9789090169125.

- Beal EJ, House CH, Orphan VJ. (2009). Manganese- and iron-dependent marine methane oxidation. *Science* **325**: 184–187.
- Beal EJ, Claire MW, House CH. (2011). High rates of anaerobic methanotrophy at low sulfate concentrations with implications for past and present methane levels. *Geobiology* **9**: 131–139.
- Beatty JT, Overmann J, Lince MT, Manske AK, Lang AS, Blankenship RE *et al.* (2005). An obligately photosynthetic bacterial anaerobe from a deep-sea hydrothermal vent. *Proc Natl Acad Sci USA* **102**: 9306–9310.
- Bertram S, Blumenberg M, Michaelis W, Siegert M, Krüger M, Seifert R. (2013). Methanogenic capabilities of ANME-archaea deduced from <sup>13</sup>C-labelling approaches. *Environ Microbiol* **15**: 2384–2393.
- Blazewicz SJ, Petersen DG, Waldrop MP, Firestone MK. (2012). Anaerobic oxidation of methane in tropical and boreal soils: ecological significance in terrestrial methane cycling. *J Geophys Res Biogeosci* **117**: G02033.
- Blodau C, Deppe M. (2012). Humic acid addition lowers methane release in peats of the Mer Bleue bog, Canada. *Soil Biol Biochem* **52**: 96–98.
- Boetius A, Ravensschlag K, Schubert CJ, Rickert D, Widdel F, Gieseke A *et al.* (2000). A marine microbial consortium apparently mediating anaerobic oxidation of methane. *Nature* **407**: 623–626.
- Caporaso JG, Kuczynski J, Stombaugh J, Bittinger K, Bushman FD, Costello EK *et al.* (2010). QIIME allows analysis of high-throughput community sequencing data. *Nat Methods* **7**: 335–336.
- Chang YH, Cheng TW, Lai WJ, Tsai WY, Sun CH, Lin LH *et al.* (2012). Microbial methane cycling in a terrestrial mud volcano in eastern Taiwan. *Environ Microbiol* **14**: 895–908.
- Clesceri LS, Greenberg AE, Trussel RR (eds). (1995). *Standard Methods for the Examination of Water and Wastewater*, 19th edn. APHA-AWWA-WEF: Washington, DC, USA.
- Crowe SA, Katsev S, Leslie K, Sturm A, Magen C, Nomosatryo S *et al.* (2011). The methane cycle in ferruginous Lake Matano. *Geobiology* **9**: 61–78.
- Daims H, Bruhl A, Amann R, Schleifer KH, Wagner M. (1999). The domain-specific probe EUB338 is insufficient for the detection of all bacteria: development and evaluation of a more comprehensive probe set. *Syst Appl Microbiol* **22**: 434–444.
- Deutzmann JS, Schink B. (2011). Anaerobic oxidation of methane in sediments of Lake Constance, an oligotrophic freshwater lake. *Appl Environ Microbiol* **77**: 4429–4436.
- Egger M, Rasigraf O, Sapart CJ, Jilbert T, Jetten MSM, Rockmann T *et al.* (2015). Iron-mediated anaerobic oxidation of methane in brackish coastal sediments. *Environ Sci Technol* **49**: 277–283.
- Eller G, Kanel L, Krüger M. (2005). Cooccurrence of aerobic and anaerobic methane oxidation in the water column of Lake Plusssee. *Appl Environ Microbiol* **71**: 8925–8928.
- Ettwig KF, Shima S, van de Pas-Schoonen KT, Kahnt J, Medema MH, Op den Camp HJM *et al.* (2008). Denitrifying bacteria anaerobically oxidize methane in the absence of Archaea. *Environ Microbiol* **10**: 3164–3173.
- Ettwig KF, van Alen T, van de Pas-Schoonen KT, Jetten MSM, Strous M. (2009). Enrichment and molecular detection of denitrifying methanotrophic bacteria of the NC10 phylum. *Appl Environ Microbiol* **75**: 3656–3662.
- Ettwig KF, Butler MK, Le Paslier D, Pelletier E, Manganot S, Kuypers MMM *et al.* (2010). Nitrite-driven anaerobic methane oxidation by oxygenic bacteria. *Nature* **464**: 543–548.
- Flynn TM, Sanford RA, Ryu H, Bethke CM, Levine AD, Ashbolt NJ *et al.* (2013). Functional microbial diversity explains groundwater chemistry in a pristine aquifer. *BMC Microbiol* **13**: 146.
- Gantner S, Andersson AF, Alonso-Saez L, Bertilsson S. (2011). Novel primers for 16S rRNA-based archaeal community analyses in environmental samples. *J Microbiol Meth* **84**: 12–18.
- Girguis PR, Orphan VJ, Hallam SJ, DeLong EF. (2003). Growth and methane oxidation rates of anaerobic methanotrophic archaea in a continuous-flow bioreactor. *Appl Environ Microbiol* **69**: 5472–5482.
- Gorlenko VM. (1970). A new ohototrophic green sulphur bacterium-*Prosthecochloris aestuarii* nov. gen. nov. spec. *Z Allg Mikrobiol* **10**: 147–149.
- Grossman EL, Cifuentes LA, Cozzarelli IM. (2002). Anaerobic methane oxidation in a landfill-leachate plume. *Environ Sci Technol* **36**: 2436–2442.
- Gupta V, Smemo KA, Yavitt J, Fowle DA, Branfireun BA, Basiliko N. (2013). Stable isotopes reveal widespread anaerobic methane oxidation across latitude and peatland type. *Environ Sci Technol* **47**: 8273–8279.
- Hageman SPW, van der Weijden RD, Weijma J, Buisman CJN. (2013). Microbiological selenate to selenite conversion for selenium removal. *Water Res* **47**: 2118–2128.
- Hamady M, Walker JJ, Harris JK, Gold NJ, Knight R. (2008). Error-correcting barcoded primers for pyrosequencing hundreds of samples in multiplex. *Nat Methods* **5**: 235–237.
- Harder J. (1997). Anaerobic methane oxidation by bacteria employing <sup>14</sup>C-methane uncontaminated with <sup>14</sup>C-carbon monoxide. *Mar Geol* **137**: 13–23.
- Haroon MF, Hu SH, Shi Y, Imelfort M, Keller J, Hugenholtz P *et al.* (2013). Anaerobic oxidation of methane coupled to nitrate reduction in a novel archaeal lineage. *Nature* **500**: 567–570.
- Harrison BK, Zhang H, Berelson W, Orphan VJ. (2009). Variations in archaeal and bacterial diversity associated with the sulfate-methane transition zone in continental margin sediments (Santa Barbara Basin, California). *Appl Environ Microbiol* **75**: 1487–1499.
- Hinrichs KU, Hayes JM, Sylva SP, Brewer PG, DeLong EF. (1999). Methane-consuming archaeobacteria in marine sediments. *Nature* **398**: 802–805.
- Holmer M, Storkholm P. (2001). Sulphate reduction and sulphur cycling in lake sediments: a review. *Freshwater Biol* **46**: 431–451.
- Hu SH, Zeng RJ, Burow LC, Lant P, Keller J, Yuan ZG. (2009). Enrichment of denitrifying anaerobic methane oxidizing microorganisms. *Environ Microbiol Rep* **1**: 377–384.
- Jaeggi T, Kortman GA, Moretti D, Chassard C, Holding P, Dostal A *et al.* (2014). Iron fortification adversely affects the gut microbiome, increases pathogen abundance and induces intestinal inflammation in Kenyan infants. *Gut* **64**: 731–742.
- Jagersma GC, Meulepas RJW, Heikamp-de Jong I, Gieteling J, Klimiuk A, Schouten S *et al.* (2009). Microbial diversity and community structure of a highly active anaerobic methane-oxidizing sulfate-reducing enrichment. *Environ Microbiol* **11**: 3223–3232.
- Kappler A, Benz M, Schink B, Brune A. (2004). Electron shuttling via humic acids in microbial iron(III)



- reduction in freshwater sediment. *FEMS Microbiol Ecol* **47**: 85–92.
- Knittel K, Boetius A, Lemke A, Eilers H, Lochte K, Pfannkuche O *et al.* (2003). Activity, distribution, and diversity of sulfate reducers and other bacteria in sediments above gas hydrate (Cascadia margin, Oregon). *Geomicrobiol J* **20**: 269–294.
- Knittel K, Boetius A. (2009). Anaerobic oxidation of methane: progress with an unknown process. *Annu Rev Microbiol* **63**: 311–334.
- Lloyd KG, Lapham L, Teske A. (2006). Anaerobic methane-oxidizing community of ANME-1b archaea in hypersaline Gulf of Mexico sediments. *Appl Environ Microbiol* **72**: 7218–7230.
- Lloyd KG, Alperin MJ, Teske A. (2011). Environmental evidence for net methane production and oxidation in putative ANaerobic METHanotrophic (ANME) archaea. *Environ Microbiol* **13**: 2548–2564.
- Lösekann T, Knittel K, Nadalig T, Fuchs B, Niemann H, Boetius A *et al.* (2007). Diversity and abundance of aerobic and anaerobic methane oxidizers at the Haakon Mosby mud volcano, Barents Sea. *Appl Environ Microbiol* **73**: 3348–3362.
- Manske AK, Glaeser J, Kuypers MM, Overmann J. (2005). Physiology and phylogeny of green sulfur bacteria forming a monospecific phototrophic assemblage at a depth of 100 meters in the Black Sea. *Appl Environ Microbiol* **71**: 8049–8060.
- Martens CS, Berner RA. (1974). Methane production in interstitial waters of sulfate-depleted marine sediments. *Science* **185**: 1167–1169.
- Meulepas RJW, Jagersma CG, Khadem AF, Buisman CJN, Stams AJM, Lens PNL. (2009). Effect of environmental conditions on sulfate reduction with methane as electron donor by an Eckernforde Bay enrichment. *Environ Sci Technol* **43**: 6553–6559.
- Meulepas RJW, Jagersma CG, Zhang Y, Petrillo M, Cai H, Buisman CJN *et al.* (2010). Trace methane oxidation and the methane dependency of sulfate reduction in anaerobic granular sludge. *FEMS Microbiol Ecol* **72**: 261–271.
- Mills HJ, Hodges C, Wilson K, MacDonald IR, Sobecky PA. (2003). Microbial diversity in sediments associated with surface-breaching gas hydrate mounds in the Gulf of Mexico. *FEMS Microbiol Ecol* **46**: 39–52.
- Moran JJ, House CH, Freeman KH, Ferry JG. (2005). Trace methane oxidation studied in several Euryarchaeota under diverse conditions. *Archaea* **1**: 303–309.
- Moran JJ, House CH, Thomas B, Freeman KH. (2007). Products of trace methane oxidation during nonmethylo-trophic growth by *Methanosarcina*. *J Geophys Res-Biogeophys* **112**: G02011.
- Orphan VJ, House CH, Hinrichs KU, McKeegan KD, DeLong EF. (2001a). Methane-consuming archaea revealed by directly coupled isotopic and phylogenetic analysis. *Science* **293**: 484–487.
- Orphan VJ, Hinrichs KU, Ussler W, Paull CK, Taylor LT, Sylva SP *et al.* (2001b). Comparative analysis of methane-oxidizing archaea and sulfate-reducing bacteria in anoxic marine sediments. *Appl Environ Microbiol* **67**: 1922–1934.
- Orphan VJ, House CH, Hinrichs KU, McKeegan KD, DeLong EF. (2002). Multiple archaeal groups mediate methane oxidation in anoxic cold seep sediments. *P Natl Acad Sci USA* **99**: 7663–7668.
- Pernthaler A, Dekas AE, Brown CT, Goffredi SK, Embaye T, Orphan VJ. (2008). Diverse syntrophic partnerships from-deep-sea methane vents revealed by direct cell capture and metagenomics. *P Natl Acad Sci USA* **105**: 7052–7057.
- Quast C, Pruesse E, Yilmaz P, Gerken J, Schweer T, Yarza P *et al.* (2013). The SILVA ribosomal RNA gene database project: improved data processing and web-based tools. *Nucleic Acids Res* **41**: D590–D596.
- Raghoebarsing AA, Pol A, van de Pas-Schoonen KT, Smolders AJP, Ettwig KF, Rijpstra WIC *et al.* (2006). A microbial consortium couples anaerobic methane oxidation to denitrification. *Nature* **440**: 918–921.
- Reeburgh WS. (1976). Methane consumption in Cariaco Trench waters and sediments. *Earth Planet Sc Lett* **28**: 337–344.
- Riedinger N, Formolo MJ, Lyons TW, Henkel S, Beck A, Kasten S. (2014). An inorganic geochemical argument for coupled anaerobic oxidation of methane and iron reduction in marine sediments. *Geobiology* **12**: 172–181.
- Schreiber L, Holler T, Knittel K, Meyerdieks A, Amann R. (2010). Identification of the dominant sulfate-reducing bacterial partner of anaerobic methanotrophs of the ANME-2 clade. *Environ Microbiol* **12**: 2327–2340.
- Schubert CJ, Vazquez F, Lösekann-Behrens T, Knittel K, Tonolla M, Boetius A. (2011). Evidence for anaerobic oxidation of methane in sediments of a freshwater system (Lago di Cadagno). *FEMS Microbiol Ecol* **76**: 26–38.
- Schwertmann U, Cornell RM. (1991) Ferrihydrite In: Schwertmann U, Cornell RM (eds) *Iron Oxides in the Laboratory: Preparation and Characterization*. WILEY-VCH Verlag GmbH, pp 103–112.
- Segarra KEA, Comerford C, Slaughter J, Joye SB. (2013). Impact of electron acceptor availability on the anaerobic oxidation of methane in coastal freshwater and brackish wetland sediments. *Geochim Cosmochim Acta* **115**: 15–30.
- Segarra KEA, Schubotz F, Samarkin V, Yoshinaga MY, Hinrichs KU, Joye SB. (2015). High rates of anaerobic methane oxidation in freshwater wetlands reduce potential atmospheric methane emissions. *Nat Commun* **6**: 7477.
- Shigematsu T, Tang YQ, Kobayashi T, Kawaguchi H, Morimura S, Kida K. (2004). Effect of dilution rate on metabolic pathway shift between acetoclastic and nonacetoclastic methanogenesis in chemostat cultivation. *Appl Environ Microbiol* **70**: 4048–4052.
- Sivan O, Adler M, Pearson A, Gelman F, Bar-Or I, John SG *et al.* (2011). Geochemical evidence for iron-mediated anaerobic oxidation of methane. *Limnol Oceanogr* **56**: 1536–1544.
- Smemo KA, Yavitt JB. (2007). Evidence for anaerobic CH<sub>4</sub> oxidation in freshwater peatlands. *Geomicrobiol J* **24**: 583–597.
- Stams AJM, van Dijk JB, Dijkema C, Plugge CM. (1993). Growth of syntrophic propionate-oxidizing bacteria with fumarate in the absence of methanogenic bacteria. *Appl Environ Microbiol* **59**: 1114–1119.
- Stookey LL. (1970). Ferrozine - a new spectrophotometric reagent for iron. *Anal Chem* **42**: 779–781.
- Takeuchi M, Yoshioka H, Seo Y, Tanabe S, Tamaki H, Kamagata Y *et al.* (2011). A distinct freshwater-adapted subgroup of ANME-1 dominates active archaeal communities in terrestrial subsurfaces in Japan. *Environ Microbiol* **13**: 3206–3218.
- Timmers PHA, Gieteling J, Widjaja-Greefkes HCA, Plugge CM, Stams AJM, Lens PNL *et al.* (2015). Growth



- of anaerobic methane oxidizing archaea and sulfate reducing bacteria in a high pressure membrane-capsule bioreactor. *Appl Environ Microbiol* **81**: 1286–1296.
- van Breukelen BM, Griffioen J. (2004). Biogeochemical processes at the fringe of a landfill leachate pollution plume: potential for dissolved organic carbon, Fe(II), Mn(II), NH<sub>4</sub>, and CH<sub>4</sub> oxidation. *J Contam Hydrol* **73**: 181–205.
- van den Bogert B, de Vos WM, Zoetendal EG, Kleerebezem M. (2011). Microarray analysis and barcoded pyrosequencing provide consistent microbial profiles depending on the source of human intestinal samples. *Appl Environ Microbiol* **77**: 2071–2080.
- van Diggelen JMH, Lamers LPM, van Dijk G, Schaafsma MJ, Roelofs JGM, Smolders AJP. (2014). New insights into phosphorous mobilisation from sulphur-rich sediments: time-dependent effects of salinisation. *PLOS One* **9**: e111106.
- Vigneron A, Cruaud P, Pignet P, Caprais JC, Gayet N, Cambon-Bonavita MA *et al.* (2013). Bacterial communities and syntrophic associations involved in anaerobic oxidation of methane process of the Sonora Margin cold seeps, Guaymas Basin. *Environ Microbiol* **16**: 2777–2790.
- Wegener G, Boetius A. (2009). An experimental study on short-term changes in the anaerobic oxidation of methane in response to varying methane and sulfate fluxes. *Biogeosciences* **6**: 867–876.
- Yanagawa K, Sunamura M, Lever MA, Morono Y, Hiruta A, Ishizaki O *et al.* (2011). Niche separation of methanotrophic archaea (ANME-1 and-2) in methane-seep sediments of the eastern Japan sea offshore Joetsu. *Geomicrobiol J* **28**: 118–129.
- Yoshinaga MY, Holler T, Goldhammer T, Wegener G, Pohlman JW, Brunner B *et al.* (2014). Carbon isotope equilibration during sulphate-limited anaerobic oxidation of methane. *Nat Geosci* **7**: 190–194.
- Zehnder AJB, Brock TD. (1979). Methane formation and methane oxidation by methanogenic bacteria. *J Bacteriol* **137**: 420–432.
- Zehnder AJB, Brock TD. (1980). Anaerobic methane oxidation: occurrence and ecology. *Appl Environ Microbiol* **39**: 194–204.
- Zhang G, Jiang N, Liu X, Dong X. (2008). Methanogenesis from methanol at low temperatures by a novel psychrophilic methanogen, “*Methanobolus psychrophilus*” sp. nov., prevalent in Zoige wetland of the Tibetan plateau. *Appl Environ Microbiol* **74**: 6114–6120.
- Zhang Y, Maignien L, Zhao X, Wang F, Boon N. (2011). Enrichment of a microbial community performing anaerobic oxidation of methane in a continuous high-pressure bioreactor. *BMC Microbiol* **11**: 137.



**This work is licensed under a Creative Commons Attribution-NonCommercial-ShareAlike 4.0 International License. The images or other third party material in this article are included in the article's Creative Commons license, unless indicated otherwise in the credit line; if the material is not included under the Creative Commons license, users will need to obtain permission from the license holder to reproduce the material. To view a copy of this license, visit <http://creativecommons.org/licenses/by-nc-sa/4.0/>**

Supplementary Information accompanies this paper on The ISME Journal website (<http://www.nature.com/ismej>)